

Fracture characterization of ZEK100 magnesium alloy sheet under monotonic and non-proportional loading histories

A. Abedini, C. Butcher, M.J. Worswick

University of Waterloo, 200 University Avenue West, Waterloo, ON N2L 3G1, Canada

aabedini@uwaterloo.ca

Abstract. In the present paper, a comprehensive investigation was conducted into the fracture response of a rare-earth magnesium alloy sheet, ZEK100-O, under quasi-static conditions. Various types of specimen geometries were fabricated in different orientations with respect to the rolling direction of the sheet to reveal the anisotropic fracture response of the alloy under proportional loading conditions. To visualize directional dependency of the fracture response, experimental fracture *loci* for different orientations were constructed. Furthermore, non-proportional tests were performed by abrupt changes of stress states to study the role of the loading history on fracture behaviour of the alloy. The non-proportional tests entailed pre-straining the material in uniaxial and equi-biaxial tension up to a prescribed deformation level, followed by extreme changes of stress states to plane-strain tension or shear. Based on the results of the proportional and non-proportional tests, the validity of employing “damage indicator” approaches commonly utilized in phenomenological modelling of fracture is assessed.

1. Introduction

In recent years, there has been an increasing demand to reduce vehicle weight to tackle the global issue of green-house emissions and to meet stricter governmental eco-friendly regulations. In order to fulfil this demand, magnesium alloys can offer significant weight reduction over conventional steel or aluminum alloys. However, there are some complications associated with wide-spread adoption of magnesium alloys due to several challenges including complex anisotropic constitutive and fracture behaviour. Consequently, these alloys require broad material characterization to develop and calibrate anisotropic models. Concerning proportional loading histories, remarkable progress has been made over the past two decades in developing and refining robust experimental techniques to characterize the effect of the stress state on the onset of fracture initiation in sheet materials. These investigations have covered a range of loading conditions including the main states of shear (*e.g.* Peirs *et al.*, [1]), uniaxial tension (*e.g.* Roth and Mohr, [2]), plane-strain tension (*e.g.* Cheong *et al.*, [3]), and equi-biaxial tension (*e.g.* Koc *et al.*, [4]). These notable studies have resulted in a good understanding of the fracture response of sheet materials under monotonic loading histories. Nevertheless, understanding the behaviour of materials under non-proportional loading histories is also essential since in forming operations and crash events, materials are subjected to complex stress state changes, and non-proportionality may remarkably impact the response of materials. For instance, Graf and Hosford [5] showed that pre-straining an aluminum alloy significantly influenced its strain-based forming limit diagram (FLD). As discussed by Stoughton [6] and Stoughton and Yoon [7], adopting a stress-based



approach (stress-based FLD) can significantly reduce the path sensitivity. More recently, Marcadet and Mohr [8] investigated the influence of loading direction reversal on the onset of fracture of a DP780 steel sheet and it was reported that the strain to fracture was increased with pre-straining in compression. Despite the strong potential of magnesium alloys for light-weighting of automotive structures, they have never been thoroughly examined for their fracture response under non-proportional conditions.

The objective of the present work is to investigate the fracture behaviour of a rare-earth magnesium alloy sheet (ZEK100-O) under quasi-static conditions. To this end, the anisotropic fracture response of the material was characterized under various stress states at room temperature. The fracture *loci* of the material were constructed for different orientations with respect to the rolling direction of the sheet. Moreover, a novel test program was undertaken in which a series of severely non-proportional loading conditions were achieved that enabled experimental assessment of fracture under non-proportional stress states. Using these tests, the approach of the phenomenological models in accounting for damage accumulation was evaluated.

2. Material and Experiments

The material under investigation is a rare-earth magnesium alloy, ZEK100-O, rolled sheet with a nominal thickness of 1.55 mm. Neodymium (Nd) is the rare-earth element of the alloy that is known to randomize the texture and improve its formability. The X-ray diffraction (XRD) analysis reported in Abedini *et al.* [9] showed a spread of the basal poles along the transverse direction which is typical of rare-earth magnesium rolled sheets. The constitutive characterization performed in Abedini *et al.* [9] revealed anisotropic-asymmetric constitutive behaviour of the material. Figure 1 depicts the uniaxial tension and compression responses of ZEK100-O in different orientations. It can be seen that the yield stresses and hardening rates depend upon the test orientation. In addition, the compressive curves shown in Figure 1(b) exhibit sigmoidal shapes that are the signature of activation of twinning mechanisms to accommodate plastic deformation (Kurukuri *et al.*, [10]).

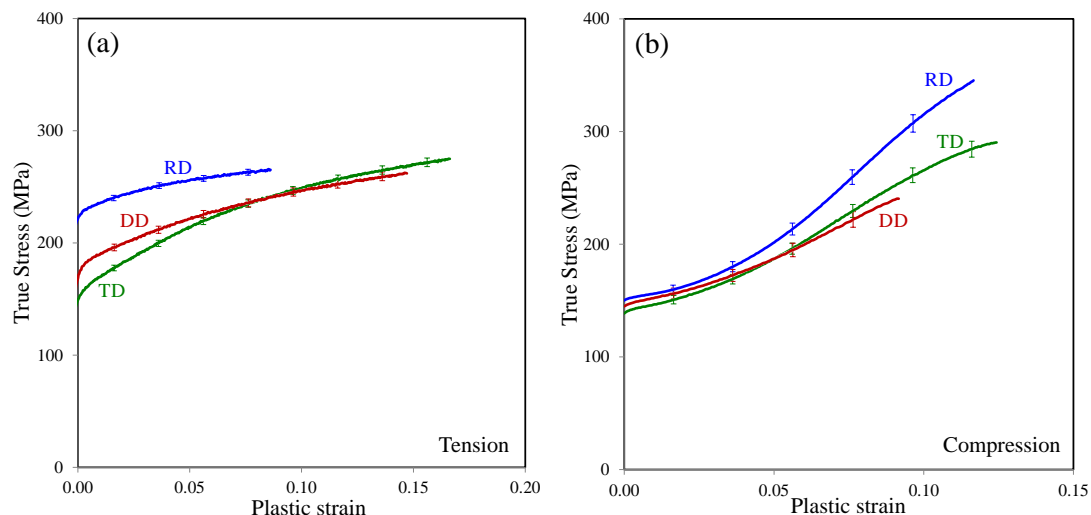


Figure 1. Stress-strain response of ZEK100-O in different orientations under (a) tension and (b) compression loading [9].

The different types of specimen geometries used in the present study for fracture characterization of the material under proportional conditions are shown in Figure 2. These specimens were extracted in different orientations with the principal directions initially aligned with the rolling (RD), diagonal (DD or 45°), or transverse (TD) directions of the sheet. It should be noted that perfectly proportional tests are usually not feasible experimentally since material or structural instabilities commonly occur

that lead to deviation from proportionality. However, in the present paper, these tests are referred to as proportional tests to differentiate them from non-proportional tests where the stress states are deliberately varied, as presented below. It is worth mentioning that all the tests described in this paper were performed under a quasi-static strain rate of 0.001 s^{-1} and at least four repeats were performed to ensure repeatability of the tests. The tests were recorded using two digital cameras for full-field stereoscopic logarithmic (Hencky) strain measurements using digital image correlation (DIC) techniques. The DIC images in each experiment were recorded with a prescribed frequency to provide approximately 300 images from the initial deformation up to fracture.

Depending upon the size of the specimens, different types of lenses were utilized, resulting in various image resolutions; however, a consistent virtual strain gauge length (VSGL) of 0.3 mm was used for all the tests. The fracture strains were reported using the last image before fracture by averaging strains of all points within a circle inspector with a diameter of 0.3 mm at the fracture initiation locations. This circle size was chosen for consistency with the VSGL size. For shear tests, strain measurements were performed using “incremental correlation” to account for large local shear strains. It should be noted that for specimen geometries that lead to significant localization, the DIC technique might be unable to accurately resolve fracture strains. In such cases, strains at fracture can be best obtained by cross-sectional area measurements of fractured specimens; however, this was left for future work. More details on experiments including equipment used to perform the tests are provided in Abedini [11].

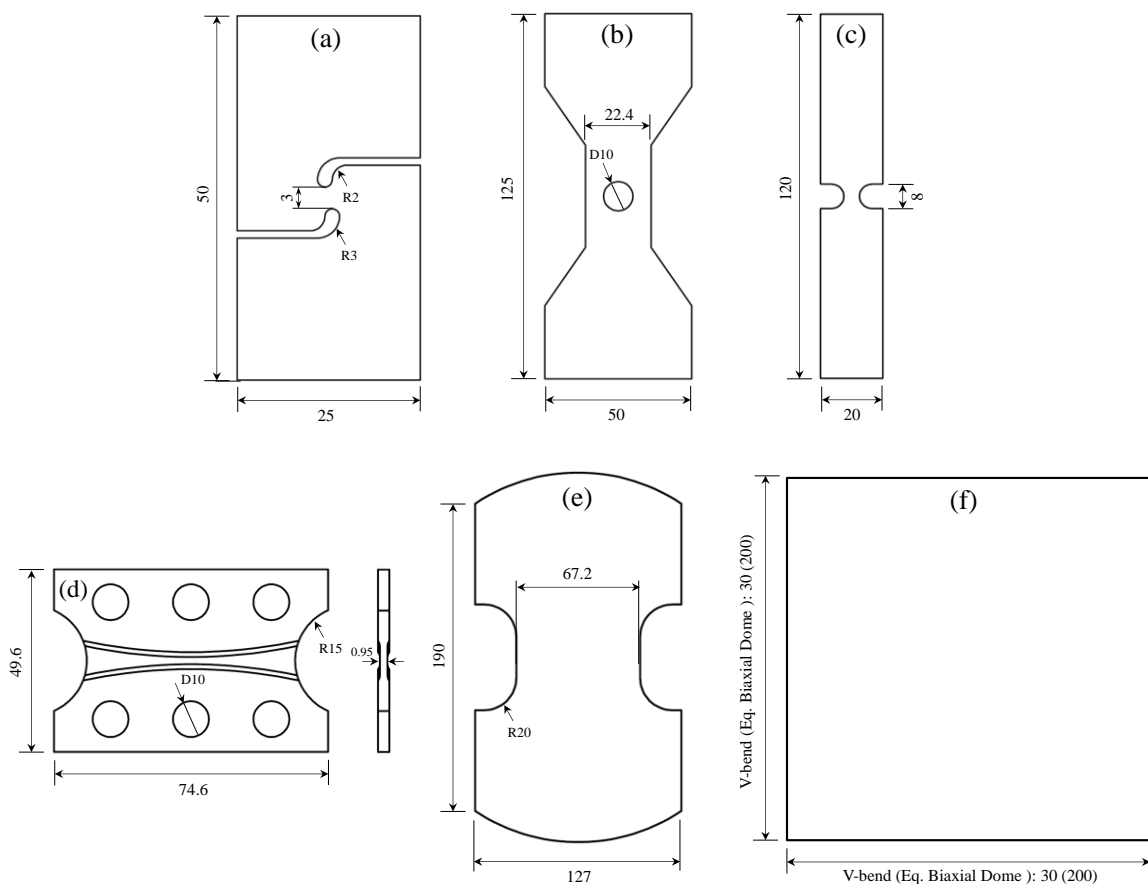


Figure 2. Specimen geometries of (a) shear, (b) hole tension, (c) notch tension, (d) butterfly, (e) plane-strain Nakazima dome, and (f) equi-biaxial Nakazima dome and v-bend tests. All dimensions are in millimetres.

To study the influence of non-proportional loading on fracture response, two-stage tests were performed to induce significant changes in the stress state. For the first stage of the loading (pre-straining), two types of specimens were used: a scaled-up tensile specimen and an equi-biaxial Marciniak specimen [11]. The first stages of deformation were stopped at a plastic work level of 22.46 MJ/m^3 that corresponds to 9% and 10% von Mises equivalent strains for uniaxial and biaxial specimens, respectively. This deformation level was chosen since it corresponds to the onset of necking in the uniaxial tension test in the RD, thus the two first stages of deformation were interrupted at the same plastic work level for consistency. Subsequently, shear and plane-strain v-bend specimens were extracted from the uniformly deformed regions of the pre-strained specimens as shown in Figure 3, and were tested to fracture using the same procedure described above.

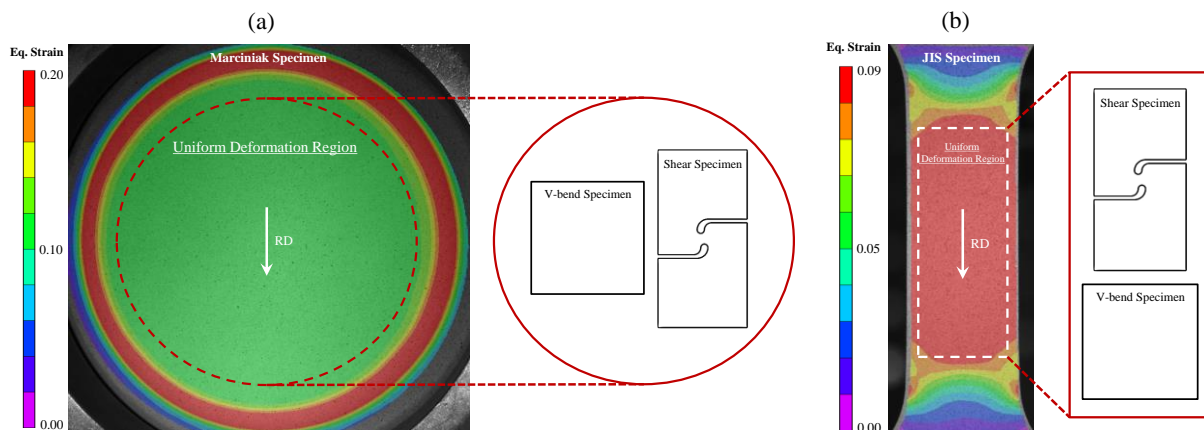


Figure 3. Shear and v-bend specimens were extracted at the end of the first stages of the non-proportional tests from the uniformly deformed regions of (a) equi-biaxial Marciniak and (b) uniaxial tensile specimens.

3. Results and Discussion

3.1. Proportional Tests

Figure 4(a) shows the strain paths to fracture for different test specimens and orientations. It can be seen that the material exhibits orientation-dependent strain paths and fracture behaviour. Anisotropy in the strain paths is more pronounced for the hole tension and notch tension tests. Of particular interest are the strain paths corresponding to the shear tests that deviate from the ideal path of equal and opposite principal strains for large strains that can be attributed to the Swift phenomenon. Moreover, Figure 4(b) shows the strain paths of all the plane-strain tests. This state is critical for sheet metal forming operations since most materials exhibit their lowest ductility under this state of deformation. It can be seen from Figure 4(b) that the strain path of the v-bend test lies almost exactly on the zero minor strain axis and the strain path of the plane-strain butterfly test is also close to the ideal path. However, the plane-strain dome test shows some deviations from an ideal plane-strain path which is due to biaxial bending associated with the punch radius. Furthermore, it can be observed that the v-bend test results in higher fracture strains than the other two tests, specifically, the fracture strains are significantly higher than those of the plane-strain butterfly test. It should be emphasized that although these experiments are referred to as plane-strain tests, they have some key differences in addition to their apparent strain path dissimilarities in Figure 4(b). For instance, bending in the v-bend test generates through-thickness stress and strain gradients that facilitate achieving higher fracture strains. As described by Min *et al.* [12], the onset of a localized necking requires every layer through the sheet thickness to exceed instability criterion. In addition, through-thickness stresses caused by contact pressure in Nakazima and v-bend tests will delay the onset of necking [12]. Also, as discussed by Abedini *et al.* [13], using through-thickness machining for specimen fabrication, increases the likelihood of initiating fracture at a local discontinuity as a result of machining-induced defects. The

butterfly specimen features a large through-thickness machined section that represents another potential reason for low fracture strains. In general, specimens that do not require through-thickness machining are more suitable for fracture characterization.

To visualize the anisotropy in fracture response of the material, a phenomenological MMC fracture curve [14] was calibrated to the experimental data in three directions corresponding to the RD, DD, and TD, shown in Figure 5. When it comes to stress state dependency, it can be seen from Figure 5 that the plane-strain tension condition has the lowest fracture strain closely followed by the shear state while the material shows the highest ductility under the uniaxial tension condition. In terms of anisotropy, it can be seen that the DD direction possesses the highest ductility while the fracture strains in the RD and TD directions are comparable. Anisotropy in fracture is most significant under the uniaxial tension condition in which the DD direction displays approximately 20% higher ductility than the RD and TD.

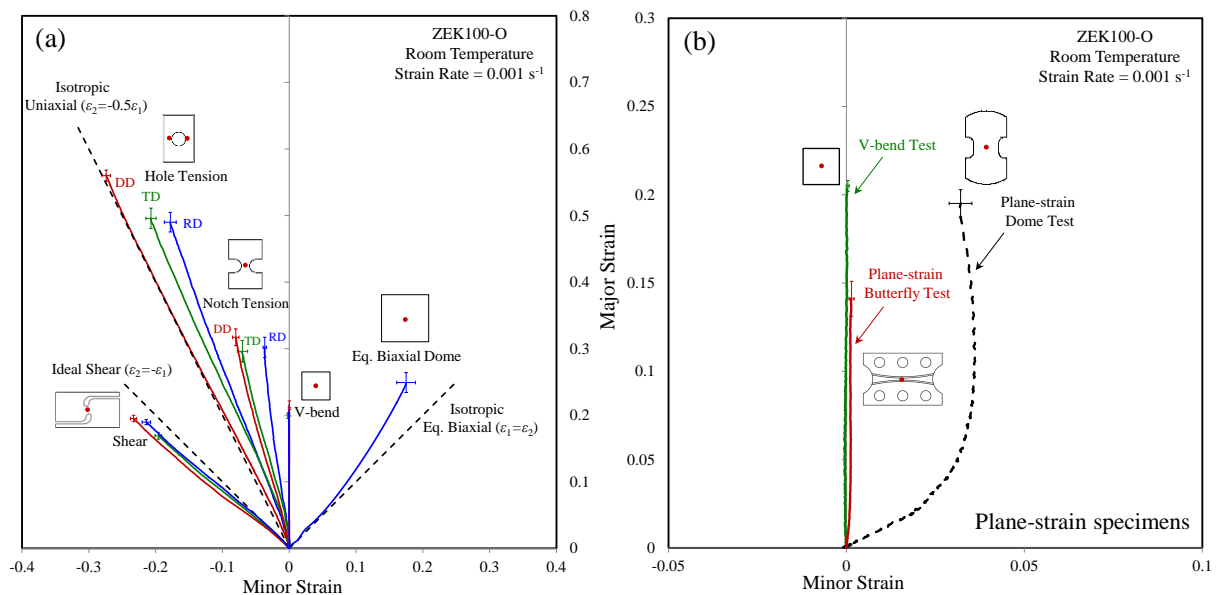


Figure 4. Strain paths to fracture for (a) different proportional tests in different orientations and (b) different plane-strain tests in the rolling direction.

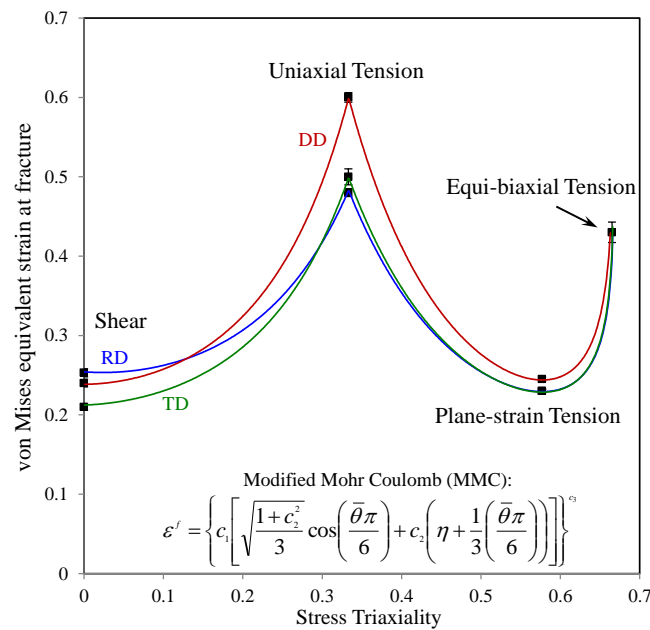


Figure 5. Fracture *loci* based on the MMC criterion [14] under proportional conditions. Symbols show the experimental data.

3.2. Non-proportional Tests

The strain paths to fracture for the non-proportional tests are shown in Figure 6(a). This figure also includes the strain paths from the initial deformation (pre-straining) up to fracture and the abrupt changes in the stress states are apparent. Moreover, the equivalent strains at fracture in the proportional and non-proportional tests are compared in Figure 6(b). Note that for the experimental results presented in Figure 6(b), the pre-strained material was treated as a “virgin material” thus the deformation corresponds only to the second stages of the loading without considering the initial strains existing in the material from the first stages of the deformation. It can be seen that the fracture strains under the shear state are not significantly affected by pre-straining; however, the fracture strains for the plane-strain tension condition are reduced by the pre-straining deformation. This reduction is more significant if pre-straining is under the equi-biaxial state.

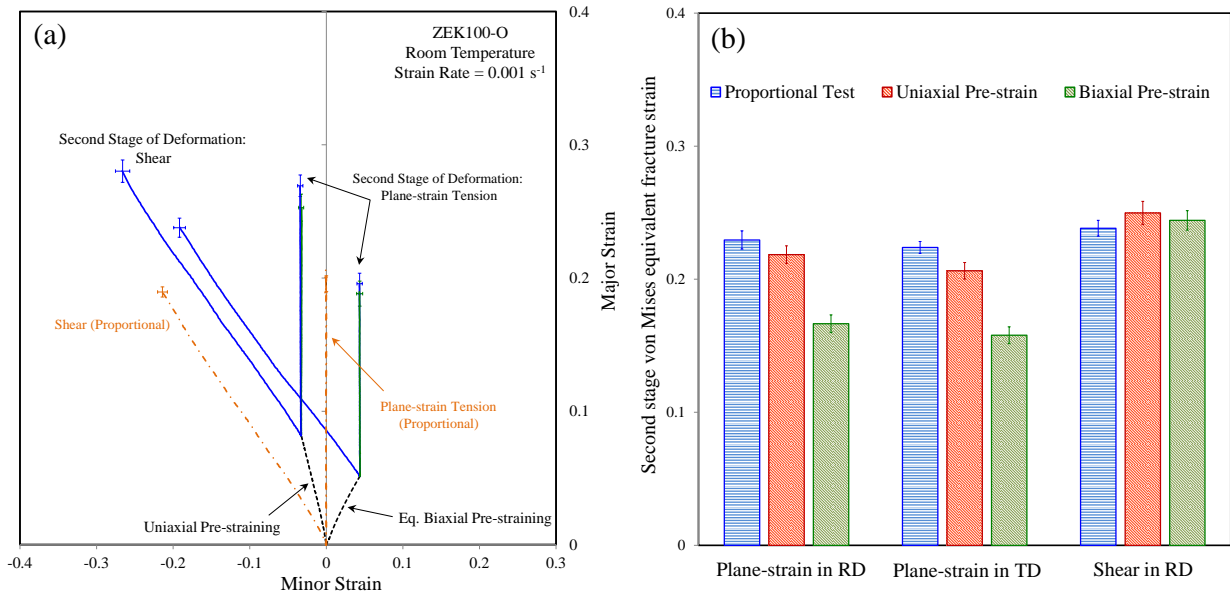


Figure 6. (a) Strain paths to fracture for non-proportional tests and (b) fracture strains under proportional and non-proportional conditions.

3.3. Damage Accumulation

A common practice in the literature, to consider non-proportionality within the phenomenological framework of fracture, is to utilize a damage indicator, D , in the form of

$$D = \left[\frac{\varepsilon^p}{\varepsilon^f(\eta, \bar{\theta})} \right]^m, \quad (1)$$

where ε^p is the equivalent plastic strain and m is the damage exponent that controls the rate of increase in D . Also ε^f is the fracture strain under proportional conditions that is a function of stress triaxiality, η , and Lode parameter $\bar{\theta}$. Note that Eq. (1) is valid for proportional conditions while for non-proportional conditions, an incremental form of Eq. (1) can be employed

$$dD = \frac{m}{\varepsilon^f(\eta, \bar{\theta})} \left[\frac{\varepsilon^p}{\varepsilon^f(\eta, \bar{\theta})} \right]^{m-1} d\varepsilon^p \quad (2)$$

To demonstrate the evolution of damage for the non-proportional tests performed in this study, Figure 7 compares the predicted fracture strains using different values of m along with the experimental data for different pre-straining conditions. It can be seen that increasing the value of the damage exponent results in better fracture predictions for the shear state for both pre-straining conditions. This is expectable because, as seen in Figure 6(b), the fracture strains in shear did not show sensitivity to pre-straining, and Eq. (1) implies that a damage exponent of infinity (no damage accumulation during pre-straining) can lead to the best fracture predictions. However, the damage exponent of $m=1.0$ and $m=1.5$ provide the best predictions for the plane-strain tension tests after biaxial and uniaxial pre-straining, respectively. It is evident from the comparison between the model predictions and measured fracture strains that no single value of damage exponent can capture the measured trends accurately.

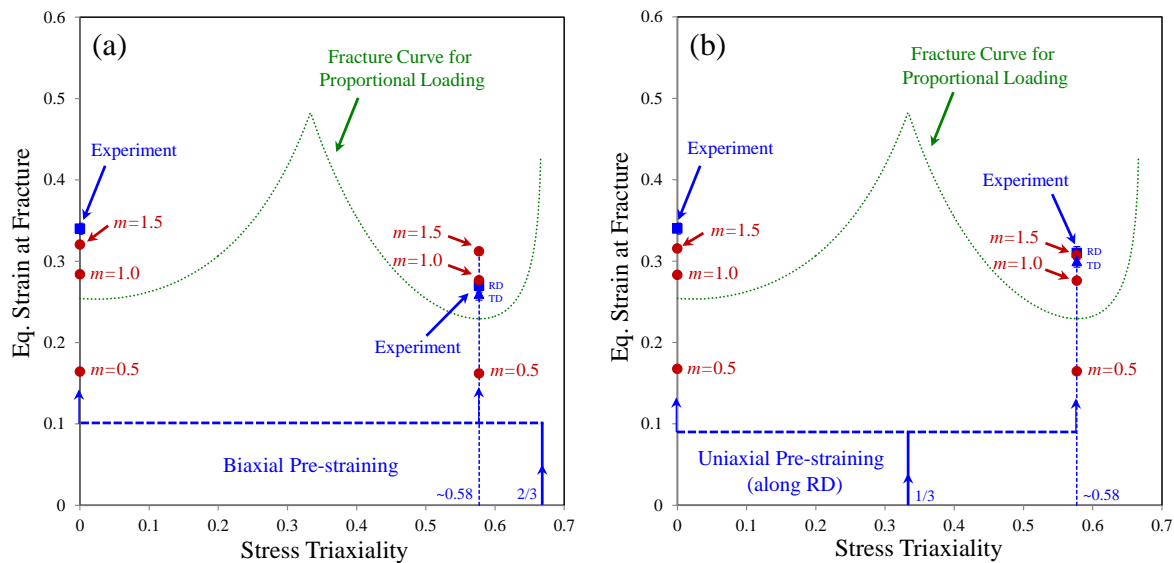


Figure 7. Influence of the damage exponent, m , on non-proportional fracture predictions with (a) biaxial pre-straining and (b) uniaxial pre-straining. Load histories are shown as blue curves. Predictions of fracture strain using the damage indicator approach for a range of damage exponents are plotted as red symbols. For reference, the proportional fracture locus in the RD is also plotted (green curve).

4. Conclusions

Fracture experiments were performed with different types of coupon-level samples extracted from a rare-earth magnesium alloy sheet to reveal the anisotropic fracture behaviour of the material. The results from the proportional loading experiments under shear, uniaxial tension, plane-strain tension, and equi-biaxial tension showed that a moderate anisotropy exists in the fracture response of the alloy. The plane-strain tension condition was achieved with different types of specimens and it was shown that the v-bend test can lead to a desired condition of almost exactly zero minor strains with the highest strains at the time of fracture. Non-proportional tests were conducted with uniaxial or biaxial pre-straining, followed by extreme changes of the stress states to plane-strain tension or shear. It was demonstrated that the fracture strains under the shear state did not show significant sensitivity to uniaxial or biaxial pre-straining histories. In other words, the shear fracture strains were similar in both the un-deformed and pre-strained materials. The fracture strains under the plane-strain state were reduced for both pre-straining conditions. The experimental design of the non-proportional experiments facilitated an analytical evaluation of the so-called damage indicator approach. It was shown that the damage indicator approach commonly employed in phenomenological fracture modelling of materials is not applicable to all stress states, at least for the material under investigation.

References

- [1] Peirs J, Verleysen P, Degrieck J 2012 Novel technique for static and dynamic shear testing of Ti6Al4V sheet. *Experimental Mechanics* vol 52 pp 729-741.
- [2] Roth C C and Mohr D 2016 Ductile fracture experiments with locally proportional loading histories, *International Journal of Plasticity* vol 79 pp 328-354.
- [3] Cheong K, Omer K, Butcher C, George R, Dykeman J 2017 Evaluation of the VDA 238-100 tight radius bending tests using digital image correlation strain measurement, *Journal of Physics: Conference Series* vol 896 pp 1-9.
- [4] Koc M, Billur E, Cora O N 2011 An experimental study on the comparative assessment of hydraulic bulge test analysis and methods, *Materials and Design* vol 32 pp 272-281.
- [5] Graf A and Hosford W F 1993 Effect of changing strain paths on forming limit diagrams of

- aluminum 2008-T4, *Metallurgical Transactions* vol 24 pp 2503-2512.
- [6] Stoughton T B 2000 A general forming limit criterion for sheet metal forming, *International Journal of Mechanical Sciences* vol 42 pp 1-42.
 - [7] Stoughton T B, Yoon J W 2011 A new approach for failure criterion for sheet metals, *International Journal of Plasticity* vol 27 pp 440-459.
 - [8] Marcadet S J and Mohr D 2015 Effect of compression-tension loading reversal on the strain to fracture of dual phase steel sheets, *International Journal of Plasticity* vol 72 pp 21-43.
 - [9] Abedini A, Butcher C, Nemcko M J, Kurukuri S, Worswick M J 2017 Constitutive characterization of a rare-earth magnesium alloy sheet (ZEK100-O) in shear loading: studies of anisotropy and rate sensitivity, *International Journal of Mechanical Sciences* vol 128-129 pp 54-69.
 - [10] Kurukuri S, Worswick M J, Bardelcik A, Mishra R K, Carter J T 2014 Constitutive behavior of commercial grade ZEK100 magnesium alloy sheet over a wide range of strain rates, *Metallurgical and Materials Transactions A*, vol 45 pp 3321-3337.
 - [11] Abedini A 2018 Constitutive and fracture characterization of an anisotropic and asymmetric alloy sheet, PhD thesis, University of Waterloo.
 - [12] Min J, Stoughton T B, Carsley J E, Lin J 2016 Compensation for process-dependent effects in the determination of localized necking limits, *International Journal of Mechanical Sciences*, Vol 117 pp 115-134.
 - [13] Abedini A, Butcher C, Worswick M J 2017 Fracture characterization of rolled sheet alloys in shear loading: Studies of specimen geometries, anisotropy, and rate sensitivity, *Experimental Mechanics* vol 57 pp 75-88.
 - [14] Bai Y and Wierzbicki T 2010 Application of extended Mohr-Coulomb criterion to ductile fracture, *International Journal of Fracture* vol 161 pp 1-20.